Multi-stage full waveform inversion strategy for 2D elastic VTI media

Ju-Won Oh, and Tariq Alkhalifah, King Abdullah University of Science and Technology*
Dong-Joo Min, Seoul National University

Summary

One of the most important issues in the multi-parametric full waveform inversion (FWI) is to find an optimal parameterization, which helps us recover the subsurface anisotropic parameters as well as seismic velocities, with minimal tradeoff. As a result, we analyze three different parameterizations for elastic VTI media in terms of the influence of the S-waves on the gradient direction for c_{13}, the spatial coverage of gradient direction and the degree of trade-offs between the parameters. Based on the dependency results, we design a multi-stage elastic VTI FWI strategy to enhance both the spatial coverage of the FWI and the robustness to the trade-offs among the parameters as well as FWI for the c_{13} structure.

Introduction

Recently, the multi-parametric full waveform inversion (FWI) has been intensively studied, because seismic signals are affected by the viscosity and the anisotropy of subsurface medium, when they propagate through Earth (Plessix and Cao, 2011; Prieux et al., 2013; Kamath and Tsvankin, 2013; Operto et al., 2013). Particularly, incorporating anisotropic parameters in FWI is important because many sedimentary rocks induce anisotropic behavior of waves. For this reason, research has focused on analyzing the multi-parametric description of the FWI model in anisotropic media. Due to its potential efficiency, such studies were devoted mainly to the acoustic VTI assumption of the model (Gholami et al., 2013; Alkhalifah and Plessix, 2014; Alkhalifah, 2014). In contrast, research on the elastic VTI FWI for reflection data is relatively rare because of the complexity of the influence of S-waves on gradient direction for c_{13} and increased of number of parameters to be considered. The former causes reverse update of elastic VTI for c_{13} when the initial S-wave velocity is inaccurate. This is because the partial derivative wavefields of c_{13} has reverse particle motion of P-P and S-S waves, which means that the total gradient direction can be positive or negative depending on the amplitude of S-waves in the data residual (Oh and Min, 2015). The other deterrent of taking the elastic nature of the wavefield into account is given by the increase in the number of parameters involved, which eventually will lead to unwanted tradeoff and poor illumination to some of the parameters. Oh and Min (2014) show that each strain induced by incidence waves determines the spatial coverage of the gradient direction and each parameter can generate the gradient direction with a wide coverage by having many types of strains in the virtual source. However, the improvement of the spatial coverage causes an increase in the potential trade-off between the parameters, because if each parameter has many types of strain as a virtual source, the radiation patterns of each parameter will resemble each other. In this abstract, we first analyze one new and two conventional parameterizations in terms of aforementioned two issues. After that, we suggest the multi-stage FWI strategy for 2D elastic VTI media to improve the FWI for c_{13}, spatial coverage of the gradient direction and trade-offs between parameters.

Inverse theory

Before introducing our multi-stage inversion strategy for the elastic VTI FWI, we first briefly explain the inverse theory. The objective function using the l_2-norm of the residuals between the modelled (u) and the field (d) data can be expressed as (Pratt et al., 1998)

$$E(\mathbf{p}) = \sum_{\omega}\sum_{s} \left\| \mathbf{u}_s(\omega,\mathbf{p}) - \mathbf{d}_s(\omega) \right\|_2^2 \quad \text{with} \tag{1}$$

$$\mathbf{u}_s(\omega,\mathbf{p}) = \mathbf{S}^{-1}(\omega,\mathbf{p})\mathbf{f}_s(\omega)\,, \tag{2}$$

where ω and s denote the angular frequency and the source, respectively, and $\mathbf{p}$ and S denote the model parameter and the modelling operator, respectively. To obtain an optimal solution minimizing the objective function, we take the partial derivative of eq. (1) with respect to the model parameter (p) and obtain the normal equation as follows:

$$\left[\sum_{\omega}\sum_{s}\left(\mathbf{J}_{s,\omega}^{T}\mathbf{J}_{s,\omega}^{*}\right)\right]\delta\mathbf{p} = \sum_{\omega}\sum_{s}\left[\mathbf{J}_{s,\omega}^{T}\left(\mathbf{d}_s(\omega)-\mathbf{u}_s(\omega,\mathbf{p})\right)^{*}\right]. \tag{3}$$

In eq. (3), $\mathbf{J}_{s,\omega}$ denotes the partial derivative wavefields (the so-called 'Jacobian'), which are generated by the following virtual source:

$$\mathbf{F}_s^{v}(\omega,\mathbf{p}) = -\frac{\mathbf{S}(\omega,\mathbf{p})}{\partial p}\mathbf{u}_s(\omega,\mathbf{p})\,, \tag{4}$$

The virtual source results from the reaction of the medium to an incidence wavefield (**u**) acting as point scatterers. To determine the complex behaviour of the elastic virtual source, Oh and Min (2014) introduced basis virtual sources, which are derived by partial derivatives of the following elastic wave equations for VTI media with respect to model parameter:

$$\rho\frac{\partial^2 u_x}{\partial t^2} = \frac{\partial}{\partial x}\left[c_{11}\frac{\partial u_x}{\partial x} + c_{13}\frac{\partial u_z}{\partial z}\right] + \frac{\partial}{\partial z}\left[c_{44}\left(\frac{\partial u_x}{\partial z}+\frac{\partial u_z}{\partial x}\right)\right] \tag{5}$$

$$\rho\frac{\partial^2 u_z}{\partial t^2} = \frac{\partial}{\partial z}\left[c_{13}\frac{\partial u_x}{\partial x} + c_{33}\frac{\partial u_z}{\partial z}\right] + \frac{\partial}{\partial x}\left[c_{44}\left(\frac{\partial u_x}{\partial z}+\frac{\partial u_z}{\partial x}\right)\right] \tag{6}$$

The u_x and u_z are the horizontal and vertical components of the wavefield, respectively.

DOI http://dx.doi.org/10.1190/segam2015-5850234.1

PG-I: For initial c_{13} and S-wave velocity

In this section, we introduce the parameter group (PG-I) for the elastic VTI FWI. As Oh and Min (2015) indicated, the c_{13} is one of the hardest parameters to invert in elastic VTI FWI, because the partial derivative wavefields of c_{13} have an opposite P-wave and S-wave motions that cause the gradient direction to be positive or negative depending on the amplitude of S-waves in the residual. To overcome this limitation, Oh and Min (2015) suggested to use the virtual source for λ in the isotropic parameterization instead of the virtual source for c_{13}. However, we notice that we can achieve the same result using two auxiliary parameters (a_1 and a_2), c_{13}, S-wave velocity and density as follows.

$$c_{11} = c_{13} + a_1 \tag{7}$$

$$c_{33} = c_{13} + a_1 - a_2 \tag{8}$$

$$c_{44} = \rho v_s^2 \tag{9}$$

By adopting two auxiliary parameters, the virtual source for c_{13} has the same form as λ in the isotropic parameterization and generates P-P dominated partial derivative wavefields. In most VTI media, c_{11} is larger than c_{33}. Therefore, we use a negative sign for a_2 to make its contribution positive. We also use the S-wave velocity as a direct parameter to be inverted, because if we invert c_{44} we need a good c_{44} estimate as well as a good density estimate for an accurate S-wave velocity. The main advantage of PG-I is that we can estimate a good initial c_{13}, as well as the S-wave velocities. However, the main uncertainty of PG-I is that we need a good c_{13}, density and two auxiliary parameters, which have less physical meaning, for the accurate P-wave velocity.

PG II: For P-wave velocity with wide coverage

The second parameter group (PG-II), which is suggested by Oh and Min (2014), uses horizontal P-wave velocity ($v_{p,H}$), one of Thomsen's parameters (ε), c_{13}, Poisson's ratio (σ) and density. Using the PG-II, the coefficients of the elastic wave equation can be changed as follows:

$$c_{11} = \rho v_{p,H}^2 \tag{10}$$

$$c_{33} = \frac{\rho v_{p,H}^2}{(1+2\varepsilon)} \tag{11}$$

$$c_{44} = \left(\frac{\rho v_{p,H}^2}{1+2\varepsilon}\right)\left(\frac{1-2\sigma}{2-2\sigma}\right) \tag{12}$$

As Oh and Min (2014) mentioned, the PG-II was designed to make the virtual source for each parameter to include many types of basis virtual sources. In particular, the virtual source for the horizontal P-wave velocity includes all the basis virtual sources with horizontal normal-, vertical normal- and double coupled forces. Therefore, in terms of the spatial coverage of FWI, PG-II can be the best parameterization.

However, the limitation of PG-II is that all the parameters have similar radiation pattern of partial derivative wavefields. To verify this limitation clearly, Figure 1 schematically shows the particle motions of the partial derivative wavefields induced by each basis virtual source. We only consider the horizontal component of the incidence waves when the vertical body force is applied at the surface and the subsurface point parameter is perturbed at the right side of the seismic source.

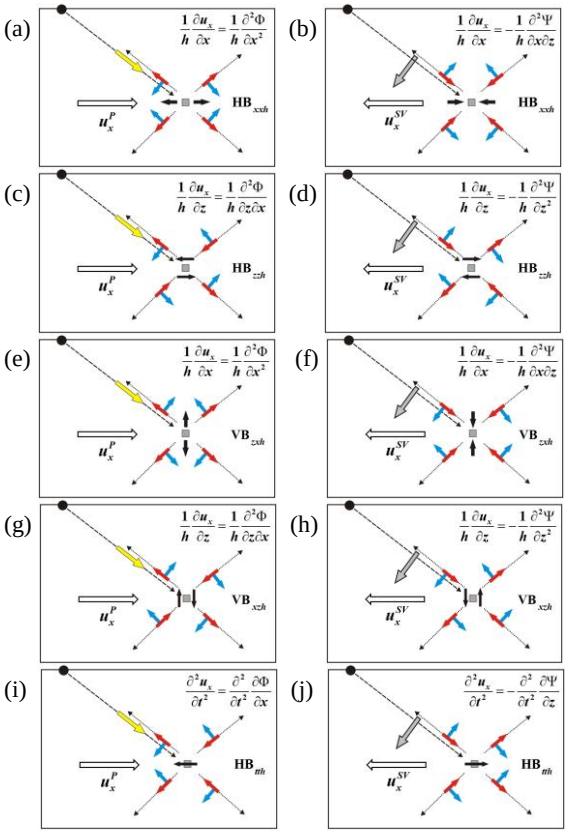

Figure 1: Scattering patterns (first particle motion) of the partial derivative wavefields for the horizontal component of the incident waves induced by each basis virtual source suggested by Oh and Min (2014). The yellow, grey, red, and blue arrows indicate the first motions of the incident P- and S-waves and the scattered P- and S-waves, respectively. The white and black arrows denote the first particle motions of the effective incident components and the first directions of corresponding basis virtual source, respectively. The equations written in the right upper side in each figure denote the momentum of each virtual source as a form of scalar (Φ) and vector (Ψ) potentials. The term h denotes a grid interval used for FWI.

These figures provide us with some insights into the trade-offs among the parameters in the multi-parametric FWI. As Oh and Min (2014) mentioned, the radiation patterns of the partial derivative wavefields for each parameter are

DOI http://dx.doi.org/10.1190/segam2015-5850234.1

determined by which types of moment sources they have in the virtual source. Accordingly, if the virtual sources for parameters have a similar combination of basis virtual sources, they behave in a similar manner during FWI, resulting in a strong trade-off, which prevents us from obtaining unique global minima solutions from the data. For this reason, we can guess that the multi-parametric FWI using PG-II suffers from severe trade-off between the parameters because most of the parameters share similar combinations of basis virtual sources.

PG-III: For less trade-off between parameters

The third parameter group (PG-III) involves four elastic coefficients and density as shown in eqs. (5) and (6). As Oh and Min (2014) showed, this parameter group has a limited spatial coverage of the gradient direction for each parameter. For this reason, many previous studies have reported that the PG-III usually fails in inverting all the parameters when the initial guess is far from the true value. However, in terms of the trade-off between parameters, PG-III provides the best set because all the parameters have totally independent basis virtual sources. In other words, the virtual sources for each parameter generate partial derivative wavefields with totally different particle motions as Figure 1 shows.

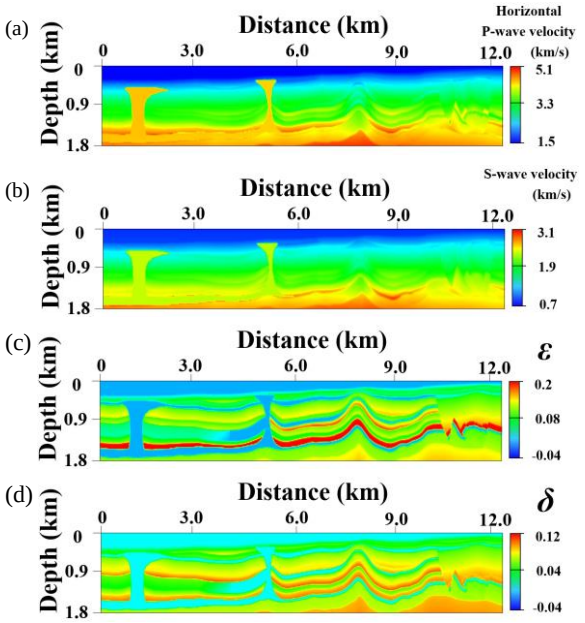

Figure 2: Downscaled version of the 2D VTI elastic BP model: (a) horizontal P-wave velocity, (b) S-wave velocity, (c) ε and (d) δ.

Multi-stage FWI strategy

Based on the characteristics of the three parameter groups, we develop a 3-stage elastic VTI FWI strategy, which starts FWI with the PG-I and then apply the PG-II and PG-III sequentially. To examine how the multi-stage FWI can improve the feasibility of the elastic VTI FWI, we perform the FWI for the downscaled version of the 2D VTI elastic BP model (Figure 2). We use the vertical P-wave velocity and Thomsen's parameters of the original BP TTI model and generate the S-wave velocity by assuming that the Poisson's ratio of the salt body equals to 0.3 and the background Poisson's ratio linearly decreases from 0.3 at the top and to 0.1 at the bottom of the model. The true density structure is generated using the empirical equation of Gardner et al. (1974). The initial models are generated based on the vertical P-wave velocity that linearly increases from 1.5 at the top to 4.2 at the bottom of the model, zero Thomsen's parameters, fixed Poisson's ratio (0.25) and the empirical equation for the density. The inversion parameters are listed on Table 1. Although we inverted all five parameters simultaneously, we only display the horizontal P-wave velocity, the S-wave velocity and two Thomsen's parameters.

Table 1: Parameters used for the FWI

Dimension	No. of shots	No. of receivers	Interval of shots	Interval of receivers	Recording time	Maximum Frequency	Minimum Frequency
12.6 km × 1.8 km	315	630	0.04 km	0.02 km	5 sec	10 Hz	0.6 Hz

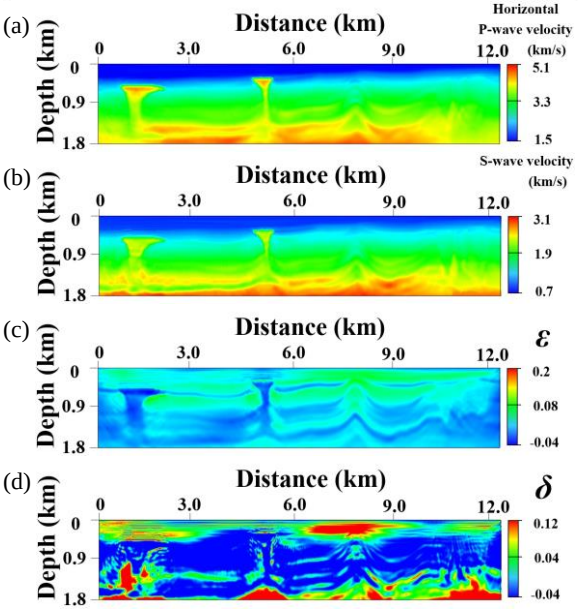

Figure 3: Inversion results obtained at 1st stage using the PG-I: (a) horizontal P-wave velocity, (b) S-wave velocity, (c) ε and (d) δ.

The purpose of the 1st stage is to prevent the reverse update of c_{13} in the early stage of FWI and to recover initial S-wave velocities for the next stage. However, as we mentioned earlier, using the PG-I does not guarantee the convergence of the P-wave velocity because three

DOI http://dx.doi.org/10.1190/segam2015-5850234.1

parameters including c_{13} and two auxiliary parameters need to be accurate. Figure 3 shows that the recovered parameters at the 1st stage using PG-I. We notice that recovered S-wave velocities are quite good while the inverted horizontal P-wave velocities are not resolved well. We also notice that the multi-parameter FWI fails to recover subsurface Thomsen's parameters. This is because of strong trade-off between these parameters in PG-I. For example, as we can guess from eqs. (7) and (8), the virtual sources for a_1 and a_2 are subsets of the virtual source for c_{13}. This means that the partial derivative wavefield of these parameters might have similar radiation patterns and it will be hard to distinguish the influence of these parameters in observed data.

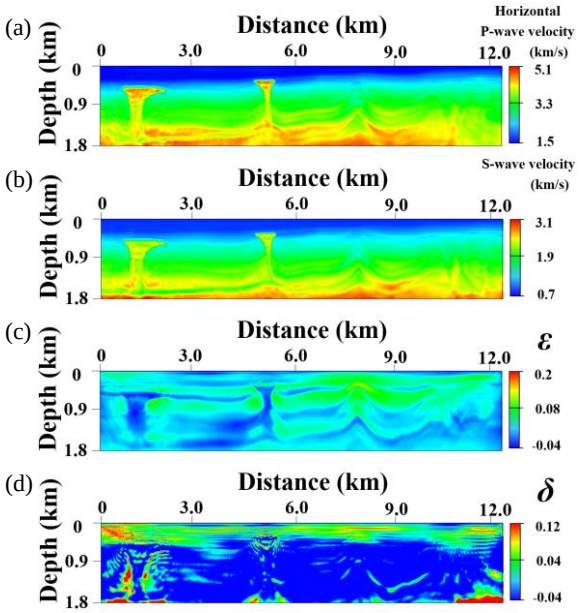

Figure 4: Inversion results obtained at 2nd stage using the PG-II based on recovered structures in Figure 3 as initial guesses: (a) horizontal P-wave velocity, (b) S-wave velocity, (c) ε and (d) δ.

Figure 4 shows the recovered parameters at 2nd stage using the PG-II. In PG-II, the horizontal P-wave velocity is a parameter in the inversion and has a wide spatial coverage of the gradient direction as we mentioned earlier. Therefore we can expect better horizontal P-wave velocity in the 2nd stage as shown in Figure 4a. However, most parameters also have similar radiation pattern because they share a similar combination of basis virtual sources. For this reason, Thomsen's parameters still suffer from strong trade-offs between the parameters (Figures 4c and 4d). Figure 5 shows the recovered structures at 3rd stage using the PG-III. Because all the parameters have independent combinations of the basis virtual sources as we can see in the elastic wave equations (5) and (6), the Thomsen's parameters start to converge to their true values.

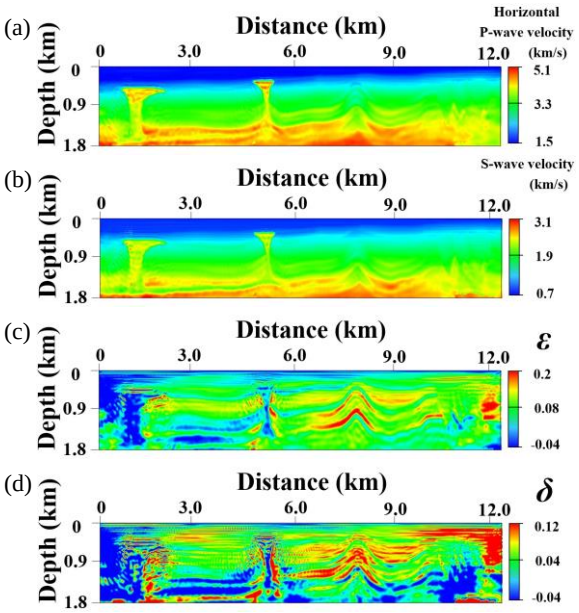

Figure 5: Inversion results obtained at 3rd stage using the PG-III based on recovered structures in Figure 4 as initial guesses: (a) horizontal P-wave velocity, (b) S-wave velocity, (c) ε and (d) δ.

Conclusions

We compare 3 elastic VTI parameterizations in terms of sensitivity to S-wave velocity in the FWI for c_{13}, spatial coverage of gradients and trade-offs among parameters. The choice of the best parameterization in elastic VTI FWI is dependent on how many prior information we have in advance of FWI. For example, if we are convinced that we have quite accurate initial P-wave and S-wave velocities, only 1-stage FWI using the PG-III (four elastic coefficients and density) will be enough to recover the subsurface anisotropy. If we are convinced that the amplitudes of S-waves in the residual wavefield is small compared to the amplitude of P-waves, we can skip the 1st stage based on PG-I, because the FWI for c_{13} might work well in that case. Otherwise, it would be optimal to utilize all 3-stages to recover both seismic velocities and anisotropic parameters.

Acknowledgments

We thank King Abdullah University of Science and Technology (KAUST) for the financial support. This work was also supported by the Human Resources Development (No.20134010200510) and Energy Efficiency & Resources Core Technology programs (No.20142510101810) of the Korea Institute of Energy Technology Evaluation and Planning (KETEP) grant funded by the Korean government Ministry of Knowledge Economy.

DOI http://dx.doi.org/10.1190/segam2015-5850234.1

EDITED REFERENCES

Note: This reference list is a copyedited version of the reference list submitted by the author. Reference lists for the 2015 SEG Technical Program Expanded Abstracts have been copyedited so that references provided with the online metadata for each paper will achieve a high degree of linking to cited sources that appear on the Web.

REFERENCES

Alkhalifah, T., 2014, Conditioning the full waveform inversion gradient to welcome anisotropy: 84th Annual International Meeting, SEG, Expanded Abstracts, 1078–1082, http://dx.doi.org/10.1190/segam2014-0120.1.

Alkhalifah, T., and R.-E. Plessix, 2014, A recipe for practical full-waveform inversion in anisotropic media: An analytical parameter resolution study: Geophysics, **79**, no. 3, R91–R101.

Gardner, G. H. F., L. W. Gardner, and A. R. Gregory, 1974, Formation velocity and density — The diagnostic basis for stratigraphic traps: Geophysics, **39**, 770–780, http://dx.doi.org/10.1190/1.1440465.

Gholami, Y., R. Brossier, S. Operto, A. Ribodetti, and J. Virieux, 2013, Which parameterization is suitable for acoustic vertical transverse isotropic full waveform? Part 1: Sensitivity and trade-off analysis: Geophysics, **78**, no. 2, R81–R105i, http://dx.doi.org/10.1190/geo2012-0204.1.

Kamath, N., and I. Tsvankin, 2013, Full-waveform inversion of multicomponent data for horizontally layered VTI media: Geophysics, **78**, no. 5, WC113–WC121, http://dx.doi.org/10.1190/geo2012-0415.1.

Oh, J. W., and D. J. Min, 2014, Multi-parametric FWI using a new parameterisation for elastic VTI media: 76th Conference & Exhibition, EAGE, Extended Abstracts, doi:10.3997/2214-4609.20141084.

Oh, J. W., and D. J. Min, 2015, A two-stage elastic FWI strategy for 2D VTI elastic media to improve c13 structure: 77th Conference & Exhibition, EAGE, Extended Abstracts, http://dx.doi.org/10.3997/2214-4609.201413408.

Operto, S., Y. Gholami, V. Prieux, A. Ribodetti, R. Brossier, L. Métivier, and J. Virieux, 2013, A guided tour of multiparameter full-waveform inversion with multicomponent data: From theory to practice: The Leading Edge, **32**, 1040–1054.

Plessix, R.-E., and Q. Cao, 2011, A parameterization study for surface seismic full waveform inversion in an acoustic vertical transversely isotropic medium: Geophysical Journal International, **185**, no. 1, 539–556, http://dx.doi.org/10.1111/j.1365-246X.2011.04957.x.

Pratt, R. G., C. Shin, and G. J. Hicks, 1998, Gauss–Newton and full Newton methods in frequency–space seismic waveform inversion: Geophysical Journal International, **133**, no. 2, 341–362, http://dx.doi.org/10.1046/j.1365-246X.1998.00498.x.

Prieux, V., R. Brossier, S. Operto, and J. Virieux, 2013, Multiparameter full waveform inversion of multicomponent ocean-bottom-cable data from the Valhall field. Part 1: Imaging compressional wave speed, density and attenuation: Geophysical Journal International, **194**, no. 3, 1640–1664, http://dx.doi.org/10.1093/gji/ggt177.